Available online at www.sciencedirect.com
SCIENCE DIRECT®
Journal of Chromatography A, 1038 (2004) 171–181
JOURNAL OF CHROMATOGRAPHY A
www.elsevier.com/locate/chroma

Evaluation and prediction of the shape of gas chromatographic peaks

P. Moretti, S. Vezzani, E. Garrone, G. Castello*

Dipartimento di Chimica e Chimica Industriale, Università di Genova, Via Dodecaneso 31, Genova I-16146, Italy

Received 28 January 2004; received in revised form 22 March 2004; accepted 22 March 2004

Available online 24 April 2004

Abstract

The evaluation and prediction of the shape of asymmetric gas chromatographic peaks is important as the knowledge of the amount of tailing permits to foresee the resolution between closely eluting peaks and to select the best analytical conditions for an efficient and rapid separation. A model function was tested in order to approximate the true peak shape obtained on non-polar column by injecting different compounds. The trend of the parameters involved in the used equation has been investigated as a function of column temperature and inlet pressure. The reproduction of the symmetrical or asymmetrical shape of gas chromatographic peaks is satisfactory and the method also permits to predict the shape of peaks obtained in different conditions of temperature and pressure.

Keywords: Peak shapes; Gas chromatography; Capillary columns; Curve fitting; Inlet pressure; Mathematical modelling

1. Introduction

Many studies of the profiles of elution peaks obtained in gas chromatography have shown that they are rarely Gaussian curves or have a symmetrical shape. Peak asymmetry is due to various intra- and extra-column mechanisms. It is therefore necessary to find a model for describing asymmetric peaks [1,2], in order to permit the reconstruction of the chromatogram and the prediction of the peak shape. Many mathematical models have been proposed in literature. A good summary of empirical functions was presented in 2001 by Di Marco and Bombi [3] and new models were published by Pap and Papai [4,5] in the same year. The most used models are described in a paper of Li [6], where the exponentially modified Gaussian (EMG) [7–9], the exponentially transformed Gaussian (ETG) [10], the polynomial modified Gaussian (PMG) [11], the generalized exponentially modified Gaussian (GEMG) [12] and a hybrid function (EGH) [13] are compared. It is often difficult to obtain an explicit equation describing the profile of the chromatographic peaks based on a rigorous physical–chemical foundation.

The elution profiles result from the interaction between various phenomena. Axial diffusion, resistance to mass transfer in the mobile phase and in the stationary phase and the unevenness of flow pattern are responsible of the increase of the peak width with increasing retention time but cannot explain the often unsymmetrical peak profiles observed. Peak tailing may be caused by other phenomena, the kinetics of adsorption–desorption [1,14–17] and by the non-linearity of the partition isotherm [18,19]. In the present work a new mathematical model is suggested which fits the peak shape in various operating conditions of pressure, temperature and amount of injected substance. The mathematical function well describes experimental chromatographic peaks and is also suitable for fitting both symmetrical and sharply ascending, slowly descending tailing peak shapes.

2. Theory

The shape of the chromatographic peak of a given compound depends on various phenomena involved in the interaction of the eluted substance along the column. When solute–solvent partition only is present in a capillary column and the analyte and the stationary phase are mutually soluble, the phenomena are: longitudinal diffusion, resistance to mass transfer between gas and liquid phase, convective mixing due to radial diffusion from the centre to the walls

* Corresponding author. Tel.: +39-010-3536176; fax: +39-010-3536199.
E-mail address: castello@chimica.unige.it (G. Castello).

0021-9673/$ – see front matter © 2004 Elsevier B.V. All rights reserved.
doi:10.1016/j.chroma.2004.03.039

of the column (this term of the Golay equation can be considered as equivalent to the eddy diffusion or multiple-path effect in packed columns). All these effects are stocastic or reversible and their sum results in a symmetrical distribution of the signal intensity. When the analyte and the liquid phase are not completely miscible, a non-linear partition isotherm is observed (negative deviation from Raoult's law), the concentration of the analyte in the liquid phase does not increase proportionally to its concentration in the mobile gas phase and as a consequence the retention time measured at the peak apex decreases with increasing amount of injected substance; the peak shows a steep front and a flat back and this kind of asymmetry starts from the peak top.

Another phenomenon influences the peak shape causing a delay in the elution of a small amount of the analyte with respect of the retention time of the bulk. In this instance the peak shows a tail in the lower part of its back. This is due to adsorption which takes place at the gas/solid interface when the liquid phase does not cover completely the capillary column wall (or the inert support in packed columns) or at the liquid/solid interface when a fraction of the analyte permeates through the liquid film and reacts with the active centres of the support or of the capillary wall. The interaction is mainly due to the formation of hydrogen bonds or other chemical bonding between the analyte (adsorbate) and the solid surface (adsorbent).

The overall effect of the adsorption is to subtract an amount of the analyte (solute) to the partition interactions with the liquid stationary phase (solvent). When adsorption is present, the peak shape is due to the sum of two contributes: a symmetrical or asymmetrical "from the top" behaviour, depending on the linear or non-linear solute–solvent partition isotherm, and a near vertical front, followed by a slow exponential decrease, due to adsoption–desorption kinetics. When the liquid phase is a good solvent for the analyte, and often also when the solute–solvent miscibility is not complete but the amount of injected sample is very small, as verified in capillary gas chromatography with high split ratio, the solute–solvent partition produces peaks which can be described by a symmetrical Gaussian distribution. When adsorption takes place, to this main symmetrical function is superimposed an asymmetric function, and the overall distribution representing the two phenomena, independent but simultaneous [20], is described by the equation:

$$y(t) = y_O \exp\left\{-\frac{1}{2(1-r^2)}[f_G^2 - 2rf_G f_A + f_A^2]\right\} \quad (1)$$

where $y(t)$ is the signal intensity at the column outlet at the time t, y_O the maximum value of the output signal, r the correlation coefficient, f_G the variable associated to the symmetrical partition distribution and f_A that associated to the asymmetrical adsorption distribution. Eq. (1) looses any significance when $r = \pm 1$. In the hypothesis that the symmetrical distribution is well represented by a normal function and that the asymmetrical one is represented by a modified log-normal function [20], with:

$$f_G = \frac{t - t_R}{\sigma_1} \quad (2)$$

$$f_A = \frac{\ln(1 + \gamma(t - t_R))}{\sigma_2} \quad (3)$$

where t_R is the time corresponding to the maximum intensity of the signal, σ_1 the dispersion of the symmetrical distribution, σ_2 the dispersion of the asymmetric distribution and γ is a parameter connected to the asymmetry value, Eq. (1) becomes:

$$y(t) = y_O \exp\left\{-\frac{1}{2(1-r^2)}\left[\frac{(t-t_R)^2}{\sigma_1^2} - 2r\frac{(t-t_R)\ln(1+\gamma(t-t_R))}{\sigma_1\sigma_2} + \frac{[\ln(1+\gamma(t-t_R))]^2}{\sigma_2^2}\right]\right\} \quad (4)$$

The used mathematical function was selected among various possible asymmetrical distribution functions because it yielded the best fit with the experimental gas chromatographic data when the amount of injected substance is small.

When the amount of injected sample increases, the added amount of analyte overcomes the adsorption capacity of the solid support or column walls, the not adsorbed fraction is only subjected to diffusion, convection and mass transfer between the gas and the liquid phase and therefore the distribution of the added amount of analyte will be described by a further normal distribution function:

$$G(t) = y_G \exp\left[-\frac{(t-t_R)^2}{2\sigma_G^2}\right] \quad (5)$$

where y_G is the peak height due to the fraction of the injected amount of sample not involved in the adsorption phenomenon, σ_G the dispersion of the symmetrical distribution.

The overall mechanism is described by the sum of Eqs. (4) and (5) and the final model function $y'(t)$ is:

$$y'(t) = y_O \exp\left\{-\frac{1}{2(1-r^2)}\left[\frac{(t-t_R)^2}{\sigma_1^2} - 2r\frac{(t-t_R)\ln(1+\gamma(t-t_R))}{\sigma_1\sigma_2} + \frac{[\ln(1+\gamma(t-t_R))]^2}{\sigma_2^2}\right]\right\} + y_G \exp\left[-\frac{(t-t_R)^2}{2\sigma_G^2}\right] \quad (6)$$

3. Experimental

The determination of the retention times and peak shape of reference mixtures containing non-polar and polar compounds was made by using a non-polar poly(dimethylsiloxane) DB-1 (J&W) capillary column with a length of

30 m × 0.32 mm i.d., phase thickness 0.25 μm, which was installed in a Varian model 3800 gas chromatograph (Varian, Palo Alto, CA, USA) equipped with a split–splitless injector and a flame ionisation detector. Helium was used as the carrier gas. The split ratio was 1/20. The inlet pressure of the column was controlled and measured by the electronic hardware of the gas chromatograph with an accuracy of ±0.1 psig (1 Pa = 1.45038×10^{-4} psig). Throughout the text the inlet pressure values are reported in psig which is the unit used for controlling and checking the gas chromatograph inlet pressure and is therefore exactly known.

Samples containing several terms of the homologous series of *n*-alkanes, of straight chain 1-alcohols and of some alkenes, chloroalkanes, ketones and others, were injected as pure compounds mixtures at the smaller amount permitted by the use of the microsyringe in order to obtain peaks of the smallest possible area, near to the detection limit of the used detector and as close as possible to the infinite dilution conditions. The analyses were carried out at temperatures between 60 and 160 °C in the inlet pressure range 5–30 psig at 2.5 psig intervals. The signal value was sampled by the data system (Varian Star) at an interval of 0.1 s for all the analyses, independent on the retention time and peak width.

4. Result and discussion

Before fitting the mathematical model to real chromatographic peak the baseline drift is corrected by subtracting the linear interpolation between the baseline values before and after the elution of the peak. The results of the proposed model function are shown in the Figs. 1-5, 10 and 11 where the residual fitting for some peaks obtained at various pressures and temperature values are also shown.

The residual shown in the figures is [21]:

$$d_i = \frac{y_{i\mathrm{cal}} - y_{i\mathrm{exp}}}{\mathrm{SDE}} \tag{7}$$

where $y_{i\,\mathrm{cal}}$ is the *i*th calculated detector signal, $y_{i\,\mathrm{exp}}$ is the corresponding experimental detector signal and the standard deviation error SDE is given by:

$$\mathrm{SDE} = \sqrt{\frac{\sum_{i=1}^{n}(y_{i\mathrm{cal}} - y_{i\mathrm{exp}})^2}{n - p}} \tag{8}$$

where *n* is the number of points of the experimental signal and *p* is the number of parameters used in the model. The model function can be considered as suitably corresponding to the experimental data when the values of the residual are in the range ±2 that corresponds to 5% significance level and do not show an increasing or decreasing trend with respect of time.

The model function of Eq. (6) was applied to the description of the shape of peaks with different asymmetry. In the case of *n*-alkanes analysed on the non-polar column, the approximately symmetrical peaks are obtained and the value of $G(t)$ of Eq. (5) therefore prevails over the term $y(t)$ of Eq. (4). The baseline noise decreases with increasing pressure and lies into the range between 1.7 μV at 30 psig and 4.0 μV at 5 psig; its actual values are shown in the captions to the figures. In Fig. 1 the experimental profile (dots) of the peak of *n*-tetradecane obtained at 100 °C and inlet pressure of 7.5 psig is compared with the line representing the calculated shape of the peak. Notwithstanding the higher noise of the signal obtained at low inlet pressure, the residual values (irregular line in the centre of the figure with values on the vertical right axis) remain well enough into the confidence range and do not show any appreciable increasing or decreasing trend. A low asymmetry value is shown by

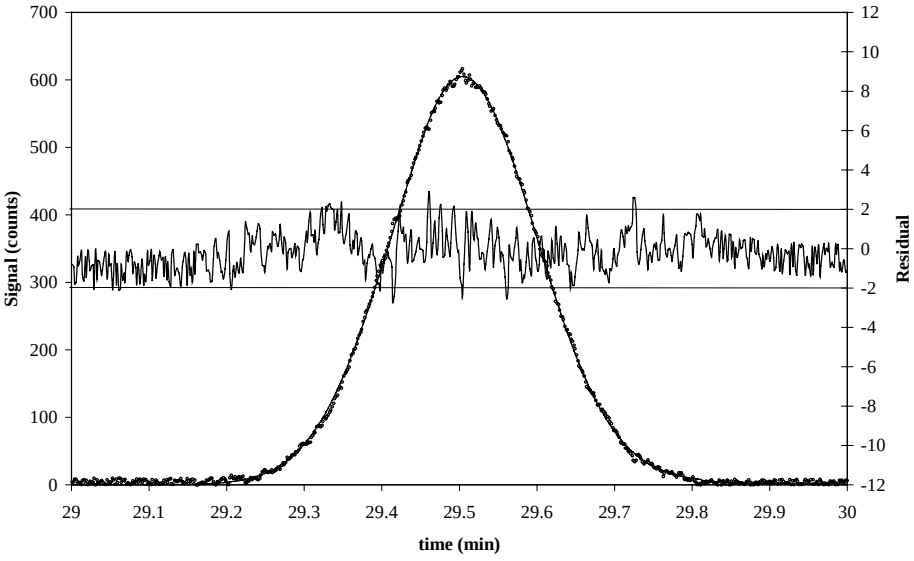

Fig. 1. Comparison of the fitting curve calculated with Eq. (6) (line) with the experimental elution peak (dots) for *n*-tetradecane on DB-1 capillary column at 100 °C and 7.5 psig (noise 2.8 μV). In the centre of the figure are plotted the residual values (right hand scale). The shape of the peak is symmetrical and the high noise influences the residual values behaviour. Values of parameters: $\gamma = 0.169\,\mathrm{s}^{-1}$; $\sigma_1 = 140.7$ s; $\sigma_2 = 3.723$; $\sigma_G = 5.747$ s; $r = 0.9987$.

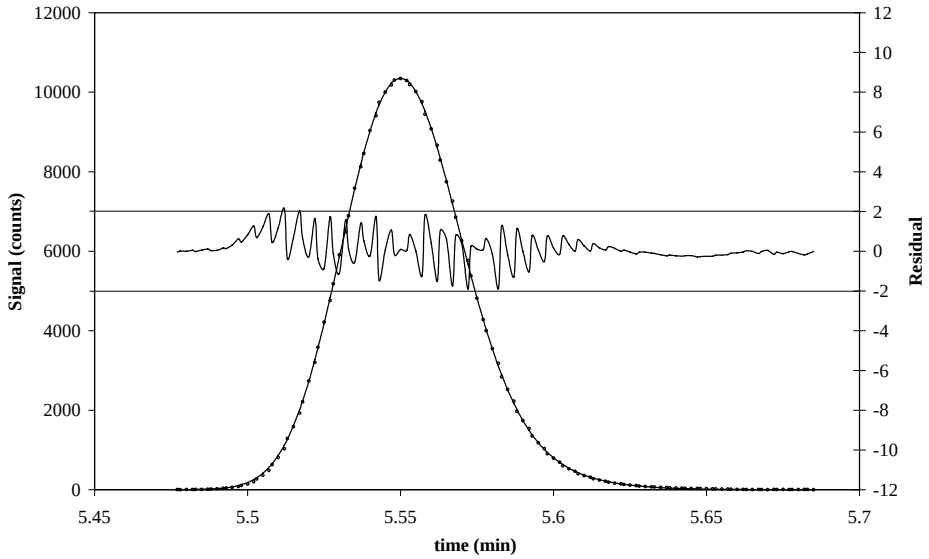

Fig. 2. Comparison of the fitting curve calculated with Eq. (6) (line) with the experimental elution peak (dots) for 1-chloroheptane on DB-1 column at 100 °C and 5 psig (noise 2.3 μV). The residual values are also plotted. The peak shows a low asymmetry. Values of parameters: $\gamma = 0.140\,s^{-1}$; $\sigma_1 = 2697$ s; $\sigma_2 = 1.120$; $\sigma_G = 1.089$ s; $r = 0.9991$.

the peaks of 1-chloroheptane. In this instance all the terms of Eq. (6) contribute to the overall calculated peak shape. Fig. 2 shows (dots) the experimental profile of the peak of 1-chloroheptane obtained at 100 °C with an inlet pressure of 5 psig; the residual values remain into the confidence range and do not show any appreciable increasing or decreasing trend. The same peak, obtained with an inlet pressure of 30 psig and a temperature of 60 °C, is shown in Fig. 3. In this instance the reconstructed peak well fits the experimental data, notwithstanding the reduced number of sample points due to the small peak width, and the residual values remain into the confidence range.

The great asymmetry shown by the 1-alcohols' peaks on the non-polar DB-1 column permitted to test the validity of the proposed function in the fitting of highly tailing peaks in presence of a great baseline noise. Fig. 4 shows the profile of the experimental peak of the 1-undecanol at 100 °C and 10 psig (dots) and the profile of the calculated peak (line). The residual values slightly overcome the confidence range due to the high baseline noise at low pressure but do not

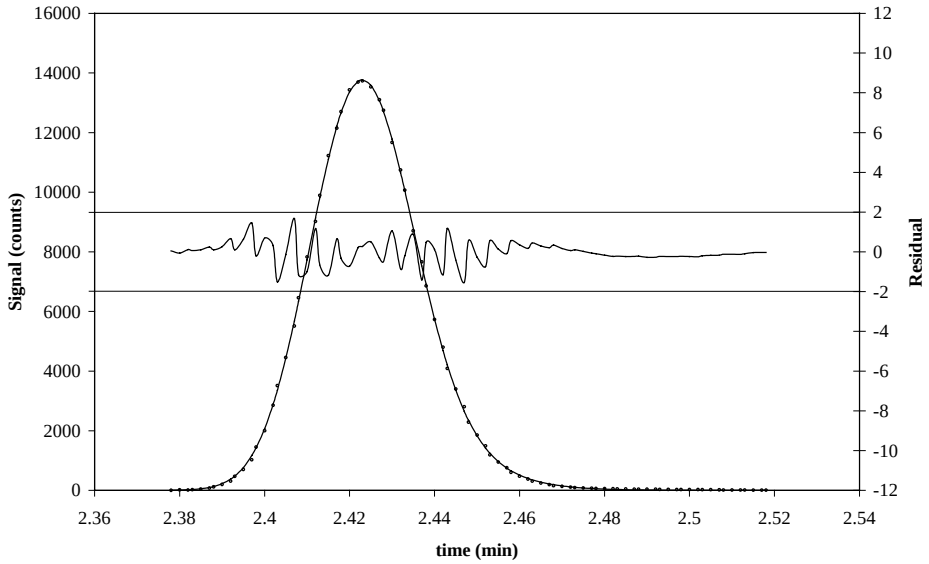

Fig. 3. Comparison of the fitting curve calculated with Eq. (6) (line) with the experimental elution peak (dots) for 1-chloroheptane on DB-1 column at 60 °C and 30 psig (noise 1.7 μV). The residual values are also plotted. The peak width is smaller than in Fig. 2. Values of parameters: $\gamma = 0.204\,s^{-1}$; $\sigma_1 = 1458.9$ s; $\sigma_2 = 1.215$; $\sigma_G = 0.703$ s; $r = 0.9990$.

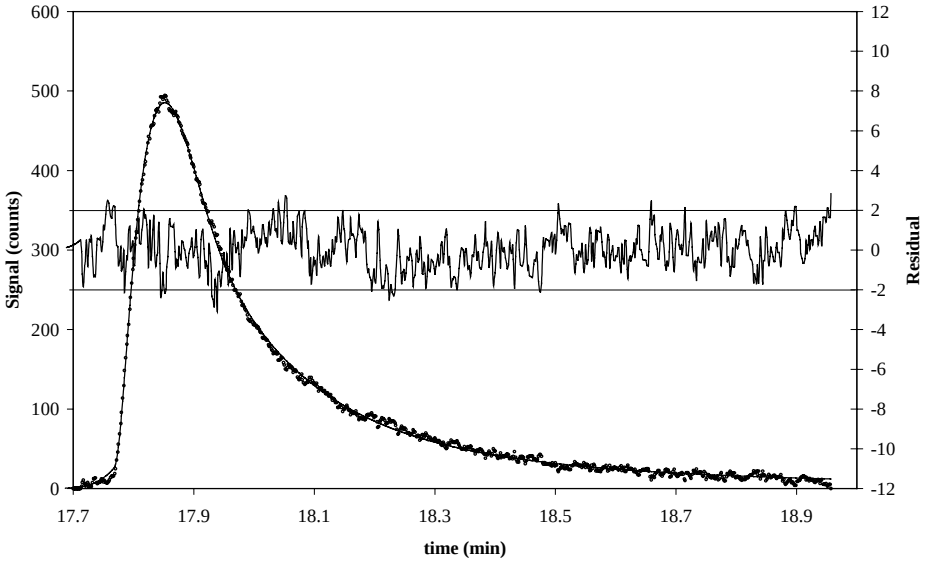

Fig. 4. Comparison of the fitting curve calculated with Eq. (6) (line) with the experimental elution peak (dots) for 1-undecanol on DB-1 column at 100 °C and 10 psig (noise 4.0 μV). The residual values are also plotted. High signal noise and great peak asymmetry were found. Values of parameters: $\gamma = 0.191\,s^{-1}$; $\sigma_1 = 780.01\,s$; $\sigma_2 = 6.133$; $\sigma_G = 3.008\,s$; $r = 0.9992$.

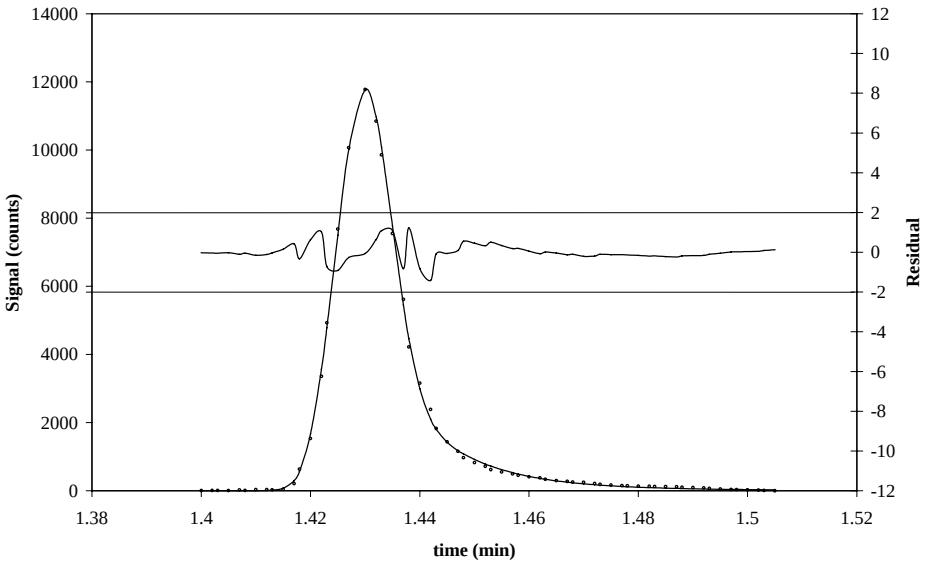

Fig. 5. Comparison of the fitting curve calculated with Eq. (6) (line) with the experimental elution peak (dots) for 1-undecanol on DB-1 column at 160 °C and 25 psig (noise 1.8 μV). The residual values are also plotted. Higher pressure decreases the noise of the signal and the peak asymmetry with respect of Fig. 4. Values of parameters: $\gamma = 1.498\,s^{-1}$; $\sigma_1 = 44.68\,s$; $\sigma_2 = 3.087$; $\sigma_G = 0.2914\,s$; $r = 0.9989$.

show any increasing or decreasing trend, notwithstanding the tail of the peak. Similar results were obtained with any inlet pressure and temperature in the range investigated. Fig. 5 shows that when the temperature is increased to 160 °C and the pressure to 25 psig the tailing decreases, the signal noise is low and the residual values remain small notwithstanding the increased slope of the signal and the smaller number of experimental points sampled with a constant sampling rate of 0.1 s (see Section 3) due to the decrease of the peak width. By examining the peak shape obtained in all the investigated analytical conditions and summarised in the reported figures, it is possible to see what phenomena may be responsible of values of the residual out of the confidence limits. It has been observed that the greatest variation of the residual values corresponds to the greatest slope of the signal near to the inflection point and to the reduced number of signal values sampled during the elution of very narrow peaks at high temperature and flow rate (Fig. 5) but the residual values fluctuation is still within the confidence limit. On the contrary, when the signal shows a high noise (Figs. 1 and 4) the residual values may be slightly outside of the confidence range. However, the proposed model function per-

Table 1
Result of the Kolmogorov–Smirnov test (see text) carried out on the peaks of different compounds at various temperatures and pressures

Compound	T (°C)	P (psig)	D_{max}	D_a
n-Tridecane	130	22.5	0.135	0.215
n-Tetradecane	100	7.5	0.033	0.070
	130	7.5	0.070	0.103
	160	25.0	0.173	0.218
1-Decanol	100	5.0	0.020	0.041
	100	7.5	0.035	0.049
1-Undecanol	100	10.0	0.022	0.048
	130	12.5	0.061	0.070
	160	25.0	0.171	0.171
1-Tridecanol	130	17.5	0.033	0.071
2-Decanone	60	30.0	0.042	0.066
1-Nonene	60	10.0	0.095	0.118
	60	30.0	0.171	0.203
1-Decene	60	30.0	0.059	0.137
1-Chloropentane	60	10.0	0.156	0.160
1-Chloroheptane	60	10.0	0.091	0.111
	60	30.0	0.137	0.148
	100	5.0	0.127	0.135
	100	10.0	0.113	0.185
1-Chlorobenzene	60	10.0	0.091	0.105
4-Methylheptane	60	10.0	0.115	0.173
2,2,5-Trimethylhexane	60	10.0	0.140	0.166
Aniline	60	10.0	0.047	0.063
	60	30.0	0.094	0.107
Naphthalene	60	30.0	0.065	0.071

mits to reconstruct the peak shape also when the acquisition of the detector signal is unpaired by rapid signal variation or by high noise.

In order to verify that the residual values obtained for the various peaks tested belong to a normal distribution, the Kolmogorov–Smirnov goodness-of-fit test (K–S test) [22] has been used. This test permits to decide if a sample comes from a population with a specific distribution and is applied to continuous distributions by comparing the observed empirical distribution function with a normal cumulative distribution function. The values for different compounds at different pressures and temperatures are shown in Table 1. D_{max} is the difference between the cumulative distribution function $F(u)$ (Gaussian) and the cumulative distribution function of the residual values $F_N(u)$, uniformly distributed in the range and D_a is the critical values. When D_{max} is smaller than D_a, the hypothesis of the normal distribution of the points of the residual is valid. In Table 1, the values corresponding to the examples shown in Figs. 1–5 are indicated, and the results of the test for all of the peaks show D_{max} values smaller than D_a, the hypothesis of the normal distribution of the residual points is confirmed and this fact enhance the validity of the proposed model. The procedure described above has shown that the proposed model permits to obtain a function which fits well the experimental values of the detector signal, when appropriate parameters are chosen and used in Eq. (6).

The parameters of Eq. (6) have been obtained with a least mean square best fit method by using the Nelder–Mead algorithm [23] and starting from the experimental behaviour of the detector signal for every peaks. The correlation coefficient, r, used in Eq. (6), was found to be approximately constant (about 0.99) in all the analyses, whereas the value of t_R was not considered as a variable parameter but taken as a constant corresponding to the peak apex, and the parameters y_O and y_G were not evaluated with respect of temperature and pressure as they are proportional to the injected amount that in the reported experiments was constant. The values of the parameters γ, σ_1, σ_2, σ_G were evaluated at three different temperature and nine pressure values, and the simplest functions capable of describing the trend of the parameters with the best fit between experimental and calculated values were selected. As an example, the equations of the func-

Table 2
Types of functions describing the trend of the parameters γ, σ_1, σ_2, σ_G and values of the coefficients, for 1-undecanol at three temperatures, used for the calculation of data shown in Figs. 6–9

Parameter	Type of function	Values of the coefficients				See figure
		T (°C)	a	b	c	
γ	$\gamma = a\ln(P) - b$	100	0.102	0.058		Fig. 6
		130	0.366	0.389		
		160	0.784	0.975		
σ_1	$\sigma_1 = a(P - b)c$	100	3931.5	3.701	−0.930	Fig.7
		130	1543.1	3.512	−1.017	
		160	1045.5	2.003	−1.039	
σ_2	$\sigma_2 = a(P)b$	100	14.883	−0.402		Fig. 8
		130	11.140	−0.349		
		160	8.023	−0.289		
σ_G	$\sigma_G = a(P)b + c$	100	132.25	−2.040	1.902	Fig. 9
		130	51.84	−1.923	0.550	
		160	23.85	−1.791	0.220	

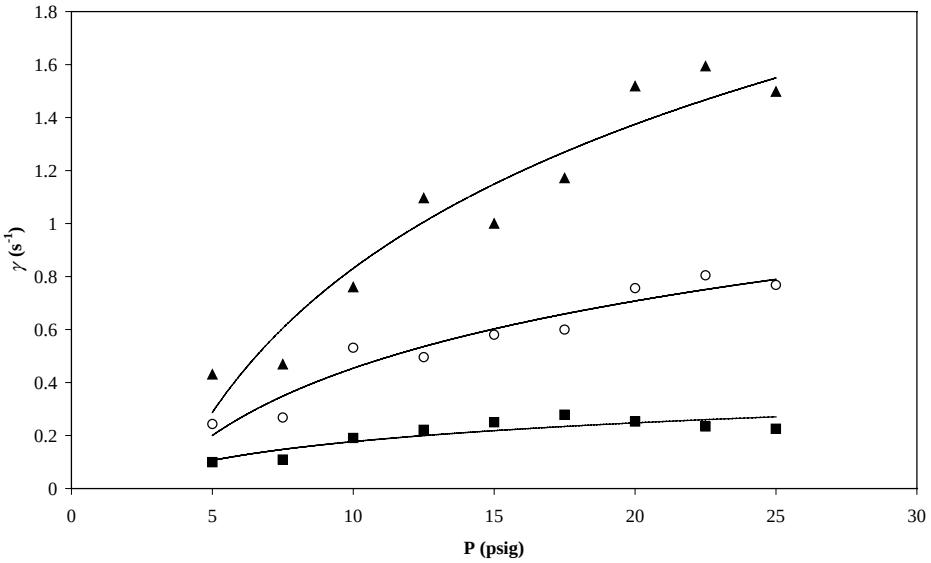

Fig. 6. Values of the parameter γ (symbols) calculated with Eq. (6) by starting from the experimental data, and interpolated trend for 1-undecanol vs. pressure at three temperatures on DB-1 column. Black triangles: $T = 160\,^{\circ}C$, white circles: $T = 130\,^{\circ}C$, black squares: $T = 100\,^{\circ}C$.

tions describing the trend of γ, σ_1, σ_2, σ_G for 1-undecanol are shown in Table 2. Fig. 6 shows the trend of the γ value of 1-undecanol as a function of pressure at three temperatures (symbols) and the calculated function which approximates the behaviour of the experimental data (lines). The γ values show a greater dispersion at the highest temperature (160 °C) due to the fact that the experimental values of the signal obtained by the data system with a constant sampling frequency of 0.1 s decrease with decreasing peak width as shown in Fig. 5. The simplest function, which approximates the trend of γ (Table 2), is of the type:

$$\gamma = a\ln(P) - b \tag{9}$$

The a and b values of this function increase with increasing temperature.

Fig. 7 shows the trend of the experimental and calculated values of σ_1 for 1-undecanol in the same conditions of pressure and temperatures as above. The values of σ_1 decrease with increasing pressure and temperature and the simplest function which approximates the trend of σ_1 is of the type:

$$\sigma_1 = a(P - b)^c \tag{10}$$

The a, b and c values of this function decrease with increasing temperature.

Fig. 8 shows the trend of the experimental and calculated σ_2 values for 1-undecanol in the same conditions of pressure

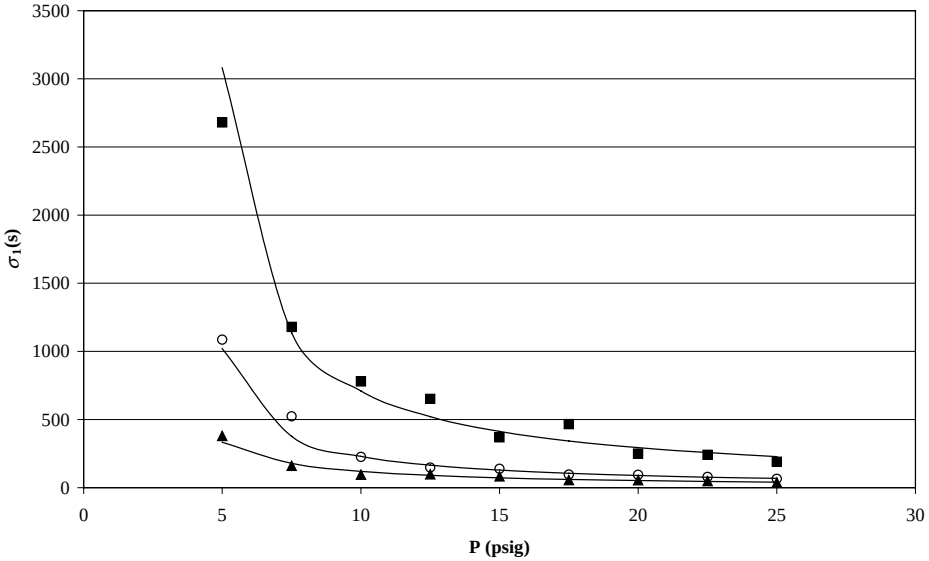

Fig. 7. Values of the parameter σ_1 (symbols) calculated with Eq. (6) by starting from the experimental data, and interpolated trend for 1-undecanol vs. pressure at three temperatures on DB-1 column. Black triangles: $T = 160\,^{\circ}C$, white circles: $T = 130\,^{\circ}C$, black squares: $T = 100\,^{\circ}C$.

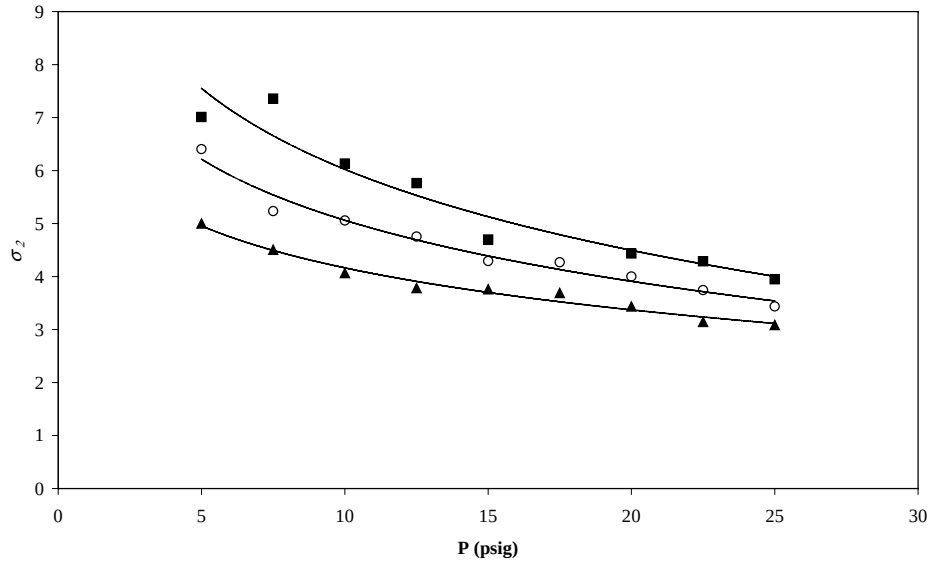

Fig. 8. Values of the parameter σ_2 (symbols) calculated with Eq. (6) by starting from the experimental data, and interpolated trend for 1-undecanol vs. pressure at three temperatures on DB-1 capillary column. Black triangles: $T = 160\,^{\circ}$C, white circles: $T = 130\,^{\circ}$C, black squares: $T = 100\,^{\circ}$C.

and temperatures as above. The simplest function, which approximates the trend of σ_1, is of the type:

$$\sigma_2 = a(P)^b \tag{11}$$

The a values of this function decrease and the b values increase with increasing temperature. Fig. 9 shows the trend of the experimental and calculated σ_G values for 1-undecanol in the same conditions of pressure and temperatures as above. The points of Fig. 9 are less scattered that those reported in the previous figures: this is due to the fact that the σ_G parameter of Eq. (9) is rather independent on the values of the other parameters, which on the contrary must be mutually correlated, in order to permit the best reconstruction of the peak shape. The simplest function, which approximates the trend of σ_G, is of the type:

$$\sigma_G = a(P)^b + c \tag{12}$$

The a and c values of this function decrease and b values increase with increasing temperature. Table 3 shows the functions and the coefficients of the parameters γ, σ_1, σ_2, σ_G obtained for other compounds at 60 °C: 1-cloroheptane, 1-nonene, 2-decanone. Independent on the compound, the

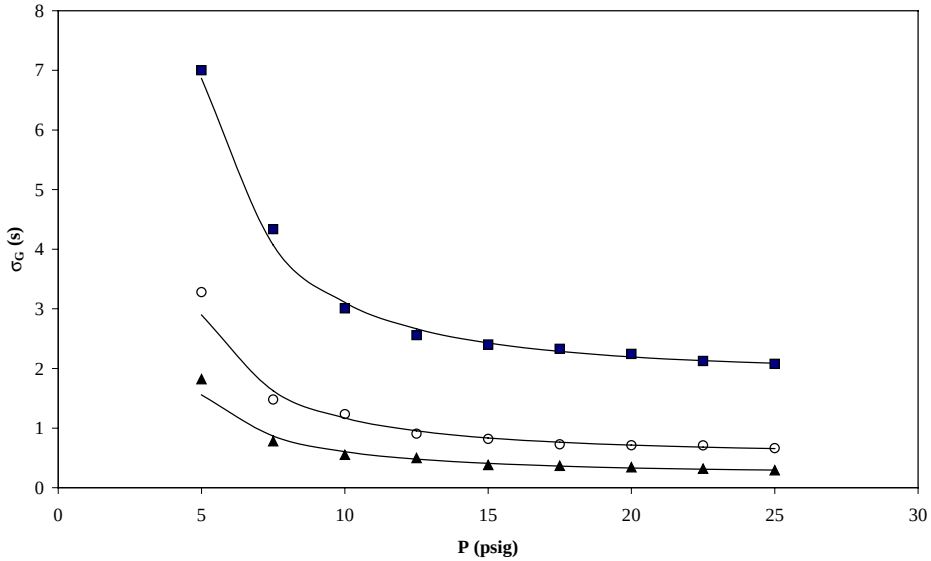

Fig. 9. Values of the parameter σ_G (symbols) calculated with Eq. (6) by starting from the experimental data, and interpolated trend for 1-undecanol vs. pressure at three temperatures on DB-1 capillary column. Black triangles: $T = 160\,^{\circ}$C, white circles: $T = 130\,^{\circ}$C, black squares: $T = 100\,^{\circ}$C.

Table 3
Types of functions describing the trend of the parameters γ, σ_1, σ_2, σ_G and values of the coefficients for 1-chloroheptane, 1-nonene and 2-decanone at 60 °C

Compound	Parameter	Type of function	Values of coefficients		
			a	*b*	*c*
1-Chloroheptane	γ	$\gamma = a\ln(P) - b$	0.091	0.025	
	σ_1	$\sigma_1 = a(P - b)c$	10.5	2.011	−0.595
	σ_2	$\sigma_2 = a(P)b$	4.121	−0.250	
	σ_G	$\sigma_G = a(P)b + c$	15.75	−1.408	0.550
1-Nonene	γ	$\gamma = a\ln(P) - b$	0.144	0.065	
	σ_1	$\sigma_1 = a(P - b)c$	6726.6	3.008	−0.651
	σ_2	$\sigma_2 = a(P)b$	47.711	−1.163	
	σ_G	$\sigma_G = a(P)b + c$	17.06	−1.703	0.502
2-Decanone	γ	$\gamma = a\ln(P) - b$	0.052	0.003	
	σ_1	$\sigma_1 = a(P - b)c$	23864.0	4.703	−0.251
	σ_2	$\sigma_2 = a(P)b$	10.688	−0.304	
	σ_G	$\sigma_G = a(P)b + c$	159.75	−1.291	7.004

type of function for each parameter is the same shown in Table 2 for 1-undecanol and only the values of *a*, *b* and *c* coefficients change.

The capacity of the proposed model to reconstruct the experimental signal value can be used in order to predict the peak shape in any analytical condition in the temperature and pressure range investigated in the preliminary runs, and with the hypothesis that the injected amount is exactly known and equal to the amount used for the determination of the parameters of Eq. (6). By interpolation of the functions of Eqs. (9)–(12), whose trend for 1-undecanol is shown in Figs. 6–9, and whose values of the coefficients *a*, *b* and *c* have been determined previously, it is possible to calculate the values of the parameters γ, σ_1, σ_2, σ_G for the considered compound at any temperature and pressure value. This permits to predict the peak shape in the new experimental conditions selected, while the retention time can be calculated by using a prediction model previously published [24]. An example of the results of the above described procedure is shown in Fig. 10. The function used for the prediction of the parameters γ, σ_1, σ_2, σ_G is of the same type shown in Table 2, but the used coefficients are obtained by using the data of three isobaric runs carried out at 10, 17.5 and 25 psig and 100 °C. By applying these functions it is possible to obtain the values of the parameters at any pressure and the peak shape can be predicted by using these values. As an example, the full line in Fig. 10 shows the predicted shape of the 1-undecanol peak at 100 °C and 12.5 psig. The points show the experimental behaviour of the detector signal obtained by injecting in the same conditions an amount

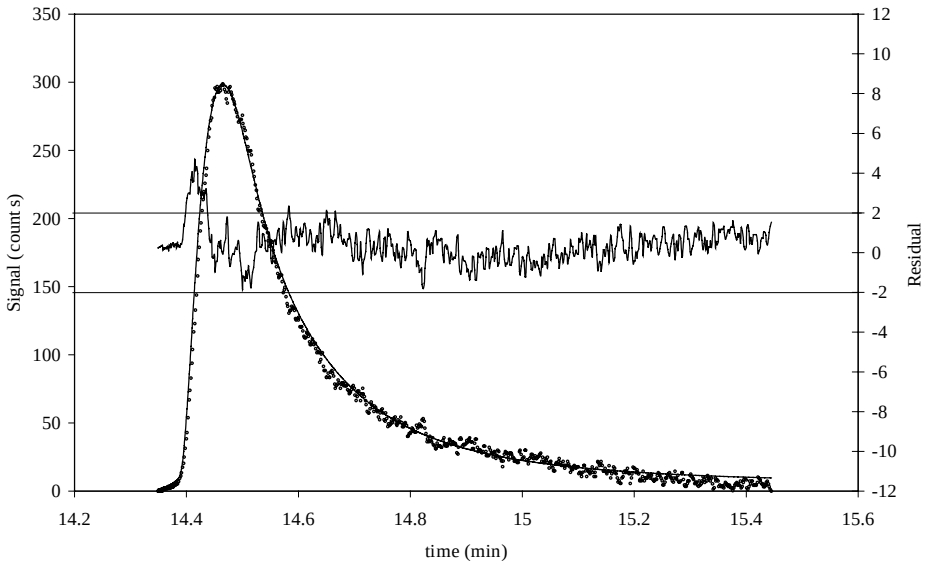

Fig. 10. Comparison of the peak shape of 1-undecanol on DB-1 column at 100 °C and 12.5 psig (noise 2.8 μV), predicted with Eq. (6) by using the γ, σ_1, σ_2, σ_G parameters calculated with preliminary runs carried out at three pressure values (10, 17.5, 25 psig) (line) with the experimental elution peak (dots). In the centre of the figure are plotted the residual values. Values of parameters: $\gamma = 0.200\,s^{-1}$; $\sigma_1 = 520.8$ s; $\sigma_2 = 5.397$; $\sigma_G = 2.666$ s; $r = 0.99$.

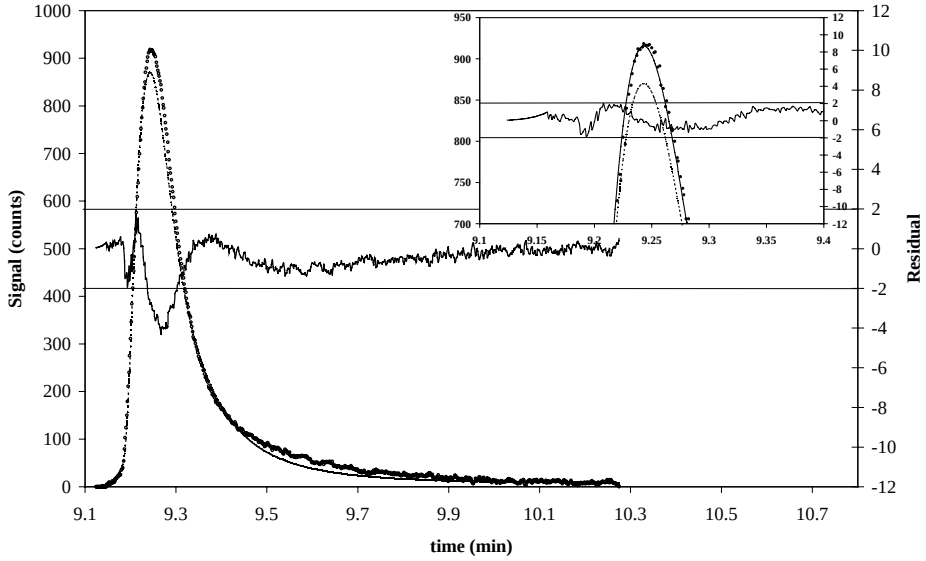

Fig. 11. Comparison of the peak shape of 1-undecanol on DB-1 column at 100 °C and 20 psig (noise 1.8 μV) predicted with Eq. (6) by using the γ, σ_1, σ_2, σ_G parameters calculated with preliminary runs at 10, 17.5, 25 psig (dashed line) and the experimental elution peak obtained by injecting an amount of sample about 5% greater than that of preliminary runs (dots). The full line was calculated by taking into account the true amount injected and better fits the experimental data (see inset). The values of the parameters are the same for both calculations: $\gamma = 0.248\,s^{-1}$; $\sigma_1 = 293.65\,s$; $\sigma_2 = 4.469$; $\sigma_G = 2.194\,s$; $r = 0.9987$.

of 1-undecanol as equal as possible to that injected in the runs used for the calculation of the parameters. The residuals values lie outside the confidence range only in the rapidly ascending peak front, but the predicted line is very close to the experimental values. When the amount of injected sample is different from that used in the preliminary runs, the correspondence between the calculated and experimental values at the peak apex decreases. Fig. 11 shows the results of analyses carried out at 100 °C and 20 psig. The prediction made in the hypothesis that the amount injected was the same of the preliminary runs results in the peak profile indicated by the dashed line, with a peak apex lower than the experimental values (dots) due to injection of an amount of sample about 5% greater. When the prediction was carried out by using the true injected amount, the calculated values (full line) better fit the experimental ones, as shown in the window of Fig. 11. In this instance all the residual values lie within the confidence limit.

The results shown in Fig. 11 indicates one of the limits of applicability of the model, because the peak shape can be exactly predicted only when the injected amount is the same of the preliminary runs or is well known in order to apply the proper corrections. By injecting different amounts of sample, it was however found that the retention time measured at the peak apex is the same independent on the peak area and height, within a reasonably large range of sample amount. This confirms the hypothesis that the overall peak shape is the sum of a symmetric curve due to reversible gas liquid solute–solvent partition to the tailing due to adsorption which only interferes with the lowest part of the peak. Therefore the retention time measured at the peak apex remains constant if the amount of sample is small enough to avoid the saturation of the liquid phase and a non-linear partition isotherm.

5. Conclusions

The proposed model is based on the reconstruction of the peak shape by the sum of adsorption phenomena with reversible solute–solvent partition. The described procedure leads to the final model equation (Eq. (6)) which represents the detector signal intensity as a function of time.

The possibility of describing with simple functions the trend of the parameters involved in the final model equation, permits to fit the shape of the peaks in any pressure and temperature condition within the range investigated with the preliminary runs. This is confirmed by the results of the different tests described above. Also the prediction of the peak shape in different analysis conditions is possible when the injected amount is the same used in the preliminary runs for the determination of the parameters or is exactly known. A further improvement of the model should take into account the effect of large variation of the injected amount, the influence of stationary phases with non-linear partition isotherm and the determination of the equation parameters for homologous series different from those tested in this work.

References

[1] A. Jaulmes, C. Vidal-Madjar, A. Ladurelli, G. Guiochon, J. Phys. Chem. 88 (1984) 5379.
[2] Zs. Papai, T.L. Pap, Analyst 127 (2000) 494.

[3] V.B. Di Marco, G.G. Bombi, J. Chromatogr. A 931 (2001) 1.
[4] T.L. Pap, Zs. Papai, J. Chromatogr. A 930 (2001) 53.
[5] Zs. Papai, T.L. Pap, J. Chromatogr. A 953 (2002) 31.
[6] J. Li, J. Chromatogr. A 952 (2002) 63.
[7] M.S. Jeansonne, J.P. Foley, J. Chromatogr. Sci. 29 (1991) 258.
[8] J.P. Foley, J.G. Dorsey, J. Chromatogr. Sci. 22 (1984) 40.
[9] I.G. McWilliam, H.C. Bolton, Anal. Chem. 43 (1971) 883.
[10] J. Li, Anal. Chem. 69 (1997) 4452.
[11] J.R. Torres-Lapasio, J.J. Baeza-Baeza, M.C. Garcia-Alvarez-Coque, Anal. Chem. 69 (1997) 3822.
[12] P. Nikitas, A. Pappa-Louisi, A. Papageorgiou, J. Chromatogr. A 912 (2001) 13.
[13] K. Lan, J.W. Jorgenson, J. Chromatogr. A 915 (2001) 1.
[14] J.C. Giddings, Anal. Chem. 35 (1963) 1999.
[15] A. Villermaux, J. Chromatogr. Sci. 12 (1974) 822.
[16] A. Cavazzini, M. Remelli, F. Dondi, A. Felinger, Anal. Chem. 71 (1999) 3453.
[17] T. Ohkuma, S. Hara, J. Chromatogr. 400 (1987) 47.
[18] F. Dondi, P. Munari, M. Remelli, A. Cavazzini, Anal. Chem. 72 (2000) 4353.
[19] G. Guiochon, S. Golshan Shirazi, A.M. Katti, Fundamentals of Preparative and Nonlinear Chromatography, Academic Press, Boston, 1994.
[20] M. Kendall, A. Stuart, Kendall's Advanced Theory of Statistics, vol. I, Arnold, London, 1990.
[21] D. Himmelblau, Process Analysis by Statistical Methods, Wiley, New York, 1970.
[22] I.M. Chakravarti, R.G. Laha, J. Roy, Handbook of Methods of Applied Statistics, vol. I, Wiley, New York, 1967, p. 392.
[23] D. Himmelblau, Applied Nonlinear Programming, Glen Head, New York, 1972.
[24] S. Vezzani, D. Pierani, P. Moretti, G. Castello, J. Chromatogr. A 848 (1999) 229.